Impact of soil moisture-climate feedbacks on CMIP5 projections: First results from the GLACE-CMIP5 experiment

Sonia I. Seneviratne,[1] Micah Wilhelm,[1] Tanja Stanelle,[1] Bart van den Hurk,[2] Stefan Hagemann,[3] Alexis Berg,[4,5] Frederique Cheruy,[6] Matthew E. Higgins,[7] Arndt Meier,[8] Victor Brovkin,[3] Martin Claussen,[3] Agnès Ducharne,[9] Jean-Louis Dufresne,[6] Kirsten L. Findell,[4] Joséfine Ghattas,[9] David M. Lawrence,[7] Sergey Malyshev,[10] Markku Rummukainen,[8] and Benjamin Smith[11]

Received 29 June 2013; revised 5 September 2013; accepted 10 September 2013.

[1] The Global Land-Atmosphere Climate Experiment–Coupled Model Intercomparison Project phase 5 (GLACE-CMIP5) is a multimodel experiment investigating the impact of soil moisture-climate feedbacks in CMIP5 projections. We present here first GLACE-CMIP5 results based on five Earth System Models, focusing on impacts of projected changes in regional soil moisture dryness (mostly increases) on late 21st century climate. Projected soil moisture changes substantially impact climate in several regions in both boreal and austral summer. Strong and consistent effects are found on temperature, especially for extremes (about 1–1.5 K for mean temperature and 2–2.5 K for extreme daytime temperature). In the Northern Hemisphere, effects on mean and heavy precipitation are also found in most models, but the results are less consistent than for temperature. A direct scaling between soil moisture-induced changes in evaporative cooling and resulting changes in temperature mean and extremes is found in the simulations. In the Mediterranean region, the projected soil moisture changes affect about 25% of the projected changes in extreme temperature. **Citation:** Seneviratne, S. I., et al. (2013), Impact of soil moisture-climate feedbacks on CMIP5 projections: First results from the GLACE-CMIP5 experiment, *Geophys. Res. Lett.*, *40*, doi:10.1002/grl.50956.

1. Introduction

[2] Recent studies have suggested that soil moisture-climate feedbacks are responsible for a substantial fraction of simulated changes in climate projections [e.g., *Seneviratne et al.*, 2006; *Boe and Terray*, 2008; *Diffenbaugh and Ashfaq*, 2010; *Boberg and Christensen*, 2012]. However, a quantification of these effects for multimodel global-scale projections has not been undertaken up to now. This is the main aim of Global Land-Atmosphere Climate Experiment–Coupled Model Intercomparison Project phase 5 (GLACE-CMIP5), a new multimodel experiment quantifying the impact of soil moisture-climate coupling in CMIP5 simulations. Compared to the previous GLACE-1 and GLACE-2 experiments [see *Koster et al.*, 2004, 2010, as well as *van den Hurk et al.*, 2011], GLACE-CMIP5 investigates long-term (decadal) rather than seasonal effects of soil moisture on climate. We present here first results of this experiment.

2. GLACE-CMIP5 Experiment

2.1. Overview of Experiment

[3] The initial phase of GLACE-CMIP5 includes two atmosphere/land only transient 1950–2100 simulations ("expA" and "expB") in which soil moisture is prescribed in the respective models according to the climatological results from a "reference" fully coupled CMIP5 simulation, covering the historical and 21st century periods (for the latter based on the RCP8.5 scenario). In cases where there were minor differences in setup (for the European-Center-Earth (EC-Earth), Geophysical Fluid Dynamics Laboratory (GFDL), and Institut Pierre-Simon Laplace (IPSL) models)—e.g., due to parameterization differences—a new reference simulation ("CTL") was computed using the prescribed sea surface temperatures (SST), sea ice, land use, and CO_2 concentrations of the respective CMIP5 simulation (Table 1). Both expA and expB simulations use prescribed SSTs, sea ice, and land use from the reference run, and the same prescribed atmospheric CO_2 concentrations (RCP8.5 CMIP5 scenario over 2006–2100 time period). The two experiments only differ in their prescribed soil moisture climatology:

[4] 1. expA: Seasonal cycle of soil moisture prescribed as 1971–2000 climatology from the reference CMIP5 coupled simulation.

[5] 2. expB: Seasonal cycle of soil moisture prescribed as a transient climatology (30 year running mean, with the exception of first 15 years using 1950–1979 climatology and last 15 years using 2071–2100 climatology) from the same reference run.

Additional supporting information may be found in the online version of this article.

[1]Institute for Atmospheric and Climate Science, ETH Zurich, Zurich, Switzerland.
[2]KNMI, De Bilt, Netherlands.
[3]Max Planck Institute for Meteorology, Hamburg, Germany.
[4]GFDL, NOAA, Princeton, New Jersey, USA.
[5]The State University of New Jersey, Rutgers, New Brunswick, New Jersey, USA.
[6]LMD/IPSL, Université Pierre et Marie Curie, Paris, France.
[7]NCAR, Boulder, Colorado, USA.
[8]Centre for Environmental and Climate Research, Lund University, Lund, Sweden.
[9]Laboratoire Sisyphe/IPSL, Université Pierre et Marie Curie, Paris, France.
[10]Princeton University, Princeton, New Jersey, USA.
[11]Department of Physical Geography and Ecosystem Science, Lund University, Lund, Sweden.

Corresponding author: S. I. Seneviratne, Institute for Atmospheric and Climate Science, ETH Zurich, CH-8092 Zurich, Switzerland. (sonia.seneviratne@env.ethz.ch)

0094-8276/13/10.1002/grl.50956

Table 1. Earth System Models (ESMs) Participating in GLACE-CMIP5

ESM Acronym	Atmospheric Model	Land Surface Model	Reference Simulation ("REF")	Reference Article(s)
CESM	National Center for Atmospheric Research Community Atmospheric Model (CAM4)	Community Land Model (CLM4)	CMIP5	*Neale et al.* [2013]; *Lawrence et al.* [2011]
EC-Earth	Integrated Forecasting System European Centre for Medium-Range Weather Forecasts	Hydrology-Tiled ECMWF Scheme for Surface Exchange over Land (H-TESSEL)	CTL (CMIP5 boundary conditions)	*Hazeleger et al.* [2011]; *Balsamo et al.* [2009]
GFDL	Geophysical Fluid Dynamics Laboratory (GFDL) Earth System Model 2 (ESM2)	Land Model 3.0 (LM3.0)	CTL (CMIP5 boundary conditions)	*Dunne et al.* [2012]; *Shevliakova et al.* [2009]
IPSL	Laboratoire de Météorologie Dynamique atmospheric model (LMDZ5A)	Organizing Carbon and Hydrology in Dynamic Ecosystems (ORCHIDEE; with two-layer soil hydrology scheme)	CTL (CMIP5 boundary conditions)	*Dufresne et al.* [2013]; *Hourdin et al.* [2013]; *Chéruy et al.* [2013]
MPI-ESM	European Centre/Hamburg forecast system	Jena Scheme for Biosphere-Atmosphere Coupling in Hamburg (JSBACH)	CMIP5	*Stevens et al.* [2013]; *Hagemann et al.* [2013]; *Raddatz et al.* [2007]; *Brovkin et al.* [2009]

[6] The differences in soil moisture in the reference, expA, and expB simulations are illustrated in Figure 1.

[7] In the present analyses, we focus on the differences between expB and expA over the time frame 2071–2100. This allows us to assess the impact of the long-term mean soil moisture changes between 1971–2000 and 2071–2100 on the late 21st century climate. Follow-up studies will consider comparisons of expA and expB with the respective CMIP5 reference simulations, including transient features of the simulations and impacts of changes in interannual soil moisture variability. The advantage of the present comparison is that it isolates the effect of changes in the soil moisture climatology (but not of changes in soil moisture variability) in the simulations, because of the minimal differences in experimental setup between expA and expB.

2.2. Participants and Analyzed Simulations

[8] Simulations with five Earth System Models (ESMs) have been contributed to GLACE-CMIP5: The Community Earth System Model (CESM), EC-Earth, GFDL, IPSL, and the Max-Planck-Institut-Earth System Model (MPI-ESM) (see Table 1 for details). All statistical quantities (mean and extremes) are computed for each model separately and results are then averaged for the main analyses. Details on the computation of extreme values are provided in the supporting information.

3. Results

[9] We focus here on both boreal (JJA) and austral (DJF) summer effects, as we find the strongest signals in midlatitude summer climate in the experiments. The analyses are provided for two regions with largest effects in these respective seasons (Figures 2 and 3). Single model analyses are provided in the supporting information (Figures S1–S8). We use the multimodel agreement as a measure of robustness in the analyses: Hatching in Figures 2 and 3 indicates regions where at least four out of five ESMs agree on the sign of change. In addition, information on the number of models with statistically significant differences is provided in the supporting information (Figure S9).

[10] The mean differences in soil moisture between expA and expB are displayed in Figures 2a and 2b. They mostly consist in reduced soil moisture, the overall features of which are consistent with analyses of changes in soil moisture availability (and agricultural drought patterns) identified in several multimodel analyses from the CMIP3 and CMIP5 archives [e.g., *Wang*, 2005; *Seneviratne et al.*, 2012; *Orlowsky and Seneviratne*, 2012, 2013]. The respective projected changes in soil moisture are mostly induced by mean changes in precipitation and evapotranspiration in the coupled reference CMIP5 simulation. In the following, we investigate how these resulting differences in mean soil moisture climatology affect late 21st century climate.

[11] We expect that first-order effects of soil moisture on the climate system are overwhelmingly driven by modifications of the turbulent heat fluxes [e.g., *Koster et al.*, 2004; *Seneviratne et al.*, 2010; *Dirmeyer*, 2011]. We thus first assess impacts on the latent and sensible heat fluxes in the experiments (Figures 2c–2f). These indeed correspond closely to the imposed differences in soil moisture in the two simulations (Figures 2a and 2b), with decreased latent and increased sensible heat fluxes in regions experiencing drier conditions in the future. The changes correspond mostly to a modified partitioning of the fluxes in the affected regions, rather than

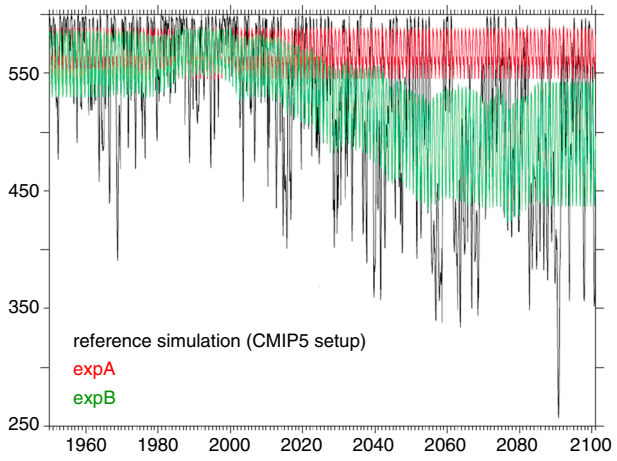

Figure 1. Illustration of experimental setup: Monthly soil moisture (mm) from 1950 to 2100 in reference simulation (black), expA (red), and expB (green) for a point in Central Europe (IPSL model).

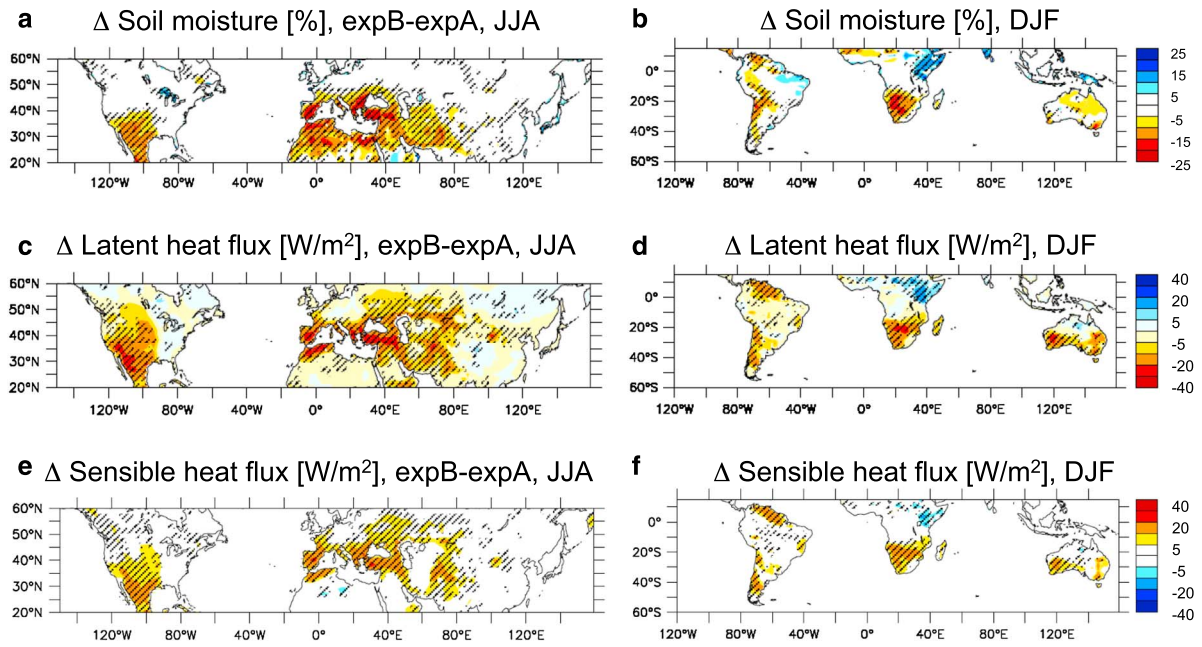

Figure 2. Difference of two experiments (expB-expA) over time period 2071–2100 for (a, b) soil moisture (% difference), (c, d) latent heat flux (W/m^2), and (e, f) sensible heat flux (W/m^2), in JJA (left; domain: 150°W:160°E, 20°N:60°N) and DJF (right; domain: 120°W:160°E, 60°S:15°N) computed as average of five model experiments. Tendencies associated with drier conditions are indicated with yellow-red shadings (lower latent heat flux, higher sensible heat flux). The plotted domains cover the regions with largest changes for the respective seasons. The hatching indicates regions in which at least four out of five models agree on the sign of change.

a change in net radiation (e.g., due to changed cloud cover), as the net sum of the turbulent fluxes is mostly unaffected in the experiments (not shown).

[12] We then analyze the impacts of the imposed soil moisture difference on temperature fields. Figures 3a–3f display differences between expB and expA in late 21st century for the average daily mean temperature (T_{mean}; Figures 3a and 3b), the average daily maximum temperature (T_{max}; Figures 3c and 3d), and the 95th percentile daily T_{max} (T_{max95}; Figures 3e and 3f), in the JJA (left) and DJF (right) seasons. The analyses reveal a substantial impact on temperature, which interestingly extends over a broader area than that directly affected by soil moisture changes and associated differences in turbulent heat fluxes in the Northern Hemisphere (Figure 2). Because the latter robust effect is often found in regions located east (i.e., downwind at midlatitudes) of those with imposed soil moisture anomalies, a possible explanation is that warm air advection leads to nonlocal soil moisture feedbacks on temperature in the simulations [see, e.g., *Vautard et al.*, 2007].

[13] The resulting temperature anomalies reach about 1–1.5 K for T_{mean}, 1.5–2 K for T_{max}, and 2–2.5 K for T_{max95} in the affected hot spots regions (see also later discussion of Fig. 4a). Note that the imposed soil moisture forcing also leads to weak cooling in some regions (e.g., tropical Eastern Africa, which is projected to experience larger precipitation amounts in the future) [see also *Shongwe et al.*, 2011].

[14] Effects on precipitation are also found, especially in the Northern Hemisphere in JJA (Figures 3g–3j). These are generally limited in absolute term for mean precipitation (P_{mean}; Figures 3g and 3h), although they are substantial in relative terms in most concerned regions (e.g., 30%–50% in the Mediterranean, see Figure S10). They are also substantial for extreme precipitation levels (95th percentile, P_{95}) in JJA (Figure 3i), although only statistically significant in a few models (see Figure S9). The net effect of enhanced soil moisture drought in the ESMs is a decrease in mean and extreme precipitation. It thus implies a strengthening of the dryness signal and a reduction of the global-scale tendency toward heavier precipitation [e.g., *Seneviratne et al.*, 2012] in the affected regions. The exact mechanism of this relationship is not clear yet but could either be related to water supply limitation or modified precipitation triggering. Nonetheless, the results are noisier and generally not robust across models in the Southern Hemisphere in DJF. Hence, the precipitation signal is mainly a feature of the Northern Hemisphere summer (but not significant in all models), possibly due to the larger continental areas in the Northern Hemisphere.

[15] An important question is the extent to which the climate response to imposed soil moisture anomalies can be considered to be approximately linear. Indeed, if such linear relationships hold, these would allow the application of observational constraints to projections in cases where models diverge in their representation of land-climate feedbacks [e.g., *Hall and Qu*, 2006; *Boberg and Christensen*, 2012]. Figure 4a displays scatter plots and linear regressions of the respective responses in T_{mean}, T_{max}, and T_{max95} versus the difference in latent heat (LH) flux based on multimodel averages (focusing only on JJA and on regions with decreased LH in future projections). Interestingly, this analysis reveals a strong linear scaling of the temperature responses to the imposed changes in latent heat flux at the surface. Changes in precipitation mean and extremes generally also show a linear scaling in the models, but the relationships are less consistent across models for precipitation than for temperature, especially for heavy precipitation (not shown).

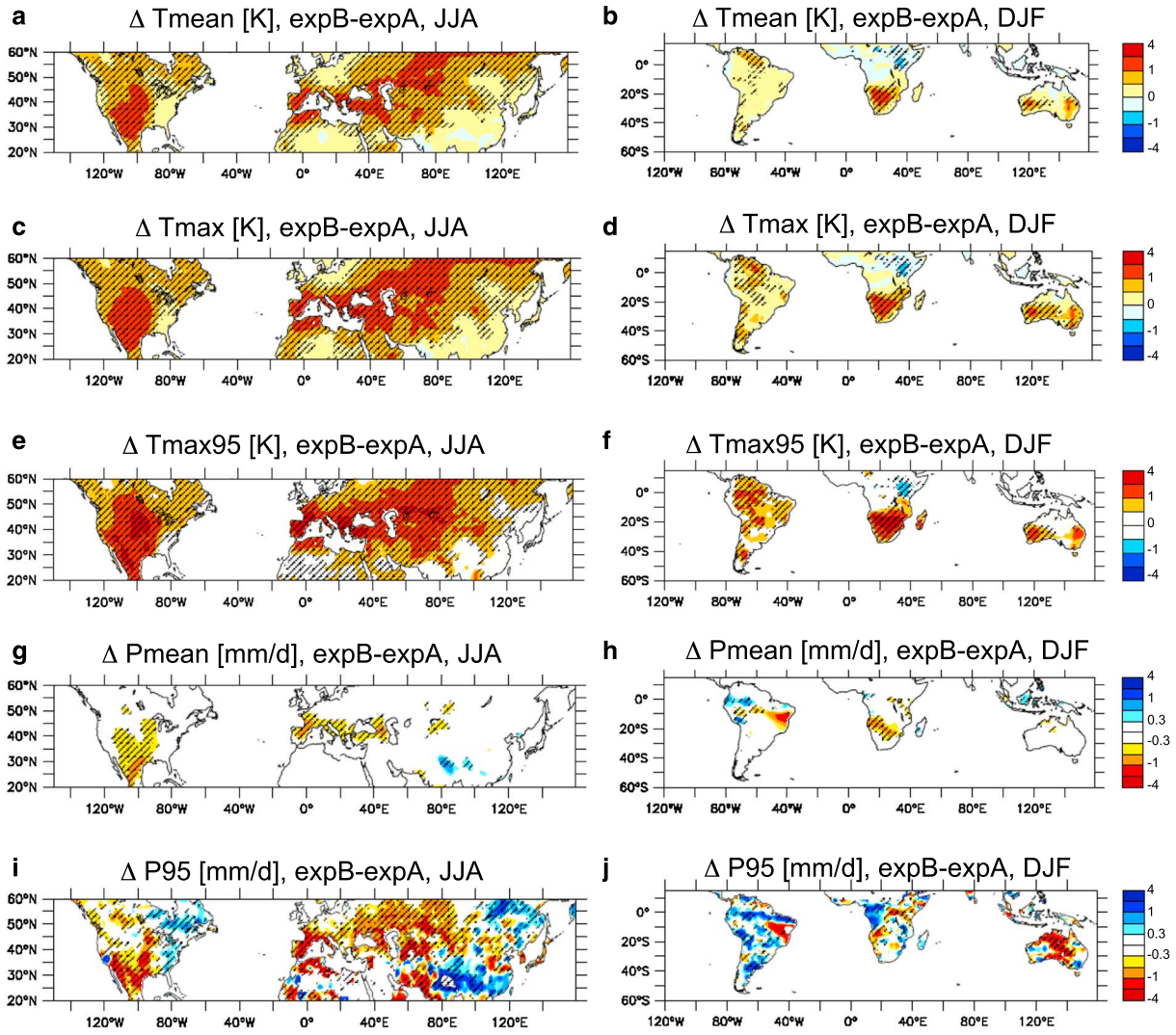

Figure 3. As Figure 2 for (a, b) mean T_{mean}, (c, d) mean T_{max}, (e, f) 95th percentile of daily T_{max}, (g, h) mean precipitation (P_{mean}), and (i j) 95th percentile of daily precipitation (P_{95}). Units are in (K) for temperature (color scale: −4, −2, −1, −0.5, 0, 0.5, 1, 2, 4) and (mm/d) for precipitation (color scale: −4, −2, −1, −0.6, −0.3, 0, 0.3, 0.6, 1, 2, 4).

[16] The respective temperature sensitivities are 0.06 K/(Wm^{-2}) for T_{mean}, 0.07 K/(Wm^{-2}) for T_{max}, and 0.08 K/(Wm^{-2}) for T_{max95}. The stronger sensitivity of T_{max} compared to that of T_{mean} can be explained by the fact that soil moisture limitation on evapotranspiration mostly affects the daytime energy balance. The finding that extreme T_{max} values are more strongly affected than mean T_{max} is consistent with observational evidence [e.g., *Hirschi et al.*, 2011; *Mueller and Seneviratne*, 2012] and supports the hypothesis that the nonlinear scaling of extreme temperature changes with global mean temperature in CMIP5 projections is related to soil moisture-temperature feedbacks [*Orlowsky and Seneviratne*, 2012].

[17] To illustrate the relevance of the identified impacts for climate change signals, Figure 4b displays the differences in T_{mean}, T_{max}, T_{max95} between late 21st century and late twentieth century for expA, expB, and the respective reference CMIP5-type simulations ("REF") in the Mediterranean region (for JJA). Overall, the signals are similar for expB and REF. Maintaining soil moisture levels at constant end of twentieth century values throughout the simulation (expA) substantially reduces the temperature signals, consistent with the results of Figures 3 and 4a. The overall effect amounts to 25% of the climate change signal for T_{max95} (respectively, 18% and 23% for T_{mean} and T_{max}). These results highlight the importance of soil moisture-climate feedbacks for regional temperature changes.

4. Summary and Conclusions

[18] This article presents first results of the GLACE-CMIP5 multimodel experiment, focusing on how projected changes in soil moisture affect projected future climate by the end of the 21st century. Substantial mean changes in soil moisture regimes take place in the climate projections between these two time periods, and these changes strongly affect regional climate (both locally and in midlatitude downwind regions), in particular for temperature mean and extremes. For precipitation, consistent (but not always statistically significant) signals are found in the simulations. There is a strong linear response of temperature to soil moisture-induced changes in evaporative cooling, with strongest effects on extremes. Given the uncertainties in the representation of soil moisture-climate feedbacks in current models [e.g., *Koster et al.*, 2004;

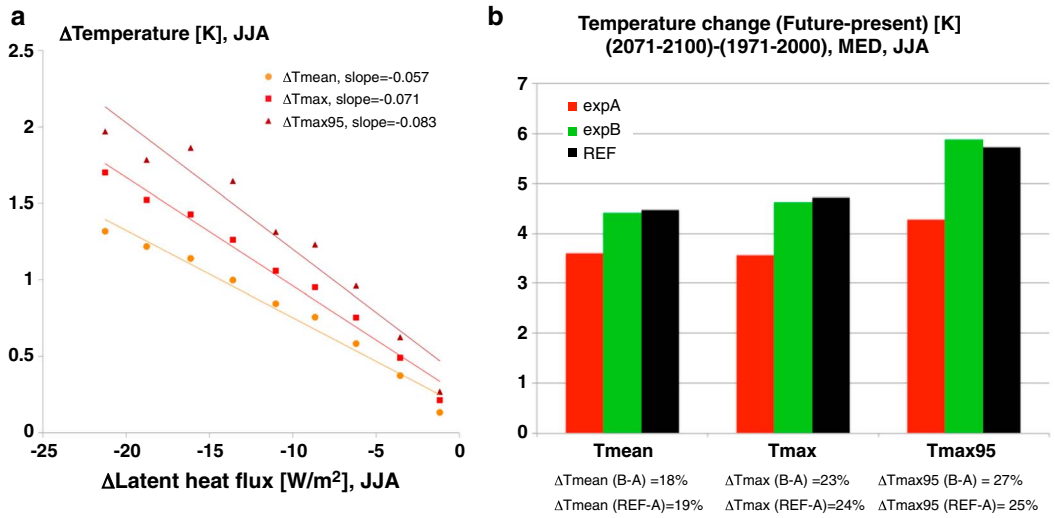

Figure 4. (a) Scatter plot and linear regressions of ΔT_{mean}, ΔT_{max}, and ΔT_{max95} versus ΔLH ($K/(Wm^{-2})$) in simulations expB-expA for JJA based on multimodel averages (domain: 150°W:160°E, 20°N:60°N; analyses only for land points and areas with negative ΔLH, using bins of 2.5 W/m^2 for ΔLH; for more details, see supporting information Discussion 4). (b) Climate change signal in expA, expB, and REF simulations over Mediterranean region in JJA (domain: 10°W:40°E, 30°N:45°N), for T_{mean}, T_{max}, and T_{max95}. The figures at the bottom of the graph indicate the differences between expB and expA (first row) and between REF and expA (second row) (%).

Dirmeyer et al., 2006; *Boe and Terray*, 2008; *Seneviratne et al.*, 2010; *Taylor et al.*, 2012; *Boberg and Christensen*, 2012] and the overall spread of climate models with respect to drought projections [*Seneviratne et al.*, 2012; *Orlowsky and Seneviratne*, 2013], these first GLACE-CMIP5 results also emphasize the need for a more in-depth evaluation of the underlying processes in existing climate models.

[19] **Acknowledgments.** The coordinators of the GLACE-CMIP5 project gratefully acknowledge support from the EU-FP7 EMBRACE project (European Commission's 7th Framework Programme, grant agreement 282672). The modeling participants (see Table 1) were able to perform the GLACE-CMIP5 simulations thanks to financial and computational support from their home institutions and/or from the institutions hosting the employed Earth System Models. A.B. was supported by the National Science Foundation (NSF) grants AGS-1035968 and AGS-1035843. A.M., M.R., and B.S. contributed through the strategic research area MERGE. We thank WCRP's GEWEX Land-Atmosphere System Study (GLASS) and IGBP's Integrated Land-Ecosystem-Atmosphere Processes Study (ILEAPS) for their sponsorship of this project. We also thank Paul Dirmeyer, Pierre Friedlingstein, Randy Koster, Chris Milly, Boris Orlowsky, Julia Pongratz, two anonymous reviewers, and the Editor for helpful comments on the modeling setup, analyses, and/or manuscript.

[20] The Editor thanks two anonymous reviewers for their assistance in evaluating this paper.

References

Balsamo, G., A. Beljaars, K. Scipal, P. Viterbo, B. van den Hurk, M. Hirschi, and A. K. Betts (2009), A revised hydrology for the ECMWF model: Verification from field site to terrestrial water storage and impact in the Integrated Forecast System, *J. Hydrometeorol.*, *10*, 623–643, doi:10.1175/2008JHM1068.1.

Boberg, F., and J. H. Christensen (2012), Overestimation of Mediterranean summer temperature projections due to model deficiencies, *Nat. Clim. Change*, *2*, 433–436, doi:10.1038/nclimate1454.

Boe, J., and L. Terray (2008), Uncertainties in summer evapotranspiration changes over Europe and implications for regional climate change, *Geophys. Res. Lett.*, *35*, L05702, doi:10.1029/2007GL032417.

Brovkin, V., T. Raddatz, C. H. Reick, M. Claussen, and V. Gayler (2009), Global biogeophysical interactions between forest and climate, *Geophys. Res. Lett.*, *36*, L07405, doi:10.1029/2009GL037543.

Chéruy, F., A. Campoy, J.-C. Dupont, A. Ducharne, F. Hourdin, M. Haeffelin, M. Chiriaco, and A. Idelkadi (2013), Combined influence of atmospheric physics and soil hydrology on the simulated meteorology at the SIRTA atmospheric observatory, *Clim. Dyn.*, *40*, 2251–2269, doi:10.1007/s00382-012-1469-y.

Diffenbaugh, N.S., and M. Ashfaq (2010), Intensification of hot extremes in the United States. *Geophys. Res. Lett.*, *37*, L15701, doi:10.1029/2010GL043888.

Dirmeyer, P.A. (2011), The terrestrial segment of soil moisture–climate coupling, *Geophys. Res. Lett.*, *38*, L16702, doi:10.1029/2011GL048268.

Dirmeyer, P. A., R. D. Koster, and Z. Guo (2006), Do global models properly represent the feedback between land and atmosphere?, *J. Hydrometeorol.*, *7*, 1177–1198.

Dufresne, J.-L., et al. (2013), Climate change projections using the IPSL-CM5 Earth System Model: from CMIP3 to CMIP5, *Clim. Dyn.*, *40*(9-10), 2123–2165, doi:10.1007/s00382-012-1636-1.

Dunne, J. P., et al. (2012), GFDL's ESM2 global coupled climate-carbon Earth System Models. Part I: Physical formulation and baseline simulation characteristics, *J. Clim.*, *25*(19), 6646–6665, doi:10.1175/JCLI-D-11-00560.1.

Hagemann, S., A. Loew, and A. Andersson (2013), Combined evaluation of MPI-ESM land surface water and energy fluxes, *J. Adv. Model. Earth Syst.*, *5*, 259–286, doi:10.1029/2012MS000173.

Hall, A., and X. Qu (2006), Using the current seasonal cycle to constrain snow albedo feedback in future climate change, *Geophys. Res. Lett.*, *33*, L03502, doi:10.1029/2005GL025127.

Hazeleger, W., et al. (2011), EC-earth V2.2: Description and validation of a new seamless Earth system prediction model, *Clim. Dyn.*, *39*, 2611–2629, doi:10.1007/s00382-011-1228-5.

Hirschi, M., S. I. Seneviratne, V. Alexandrov, F. Boberg, C. Boroneant, O. B. Christensen, H. Formayer, B. Orlowsky, and P. Stepanek (2011), Observational evidence for soil-moisture impact on hot extremes in southeastern Europe, *Nat. Geosci.*, *4*(1), 17–21.

Hourdin, F., et al. (2013), Impact of the LMDZ atmospheric grid configuration on the climate and sensitivity of the IPSL-CM5A coupled model, *Clim. Dyn.*, *40*, 2167–2192, doi:10.1007/s00382-012-1411-3.

Koster, R. D., et al. (2004), Regions of strong coupling between soil moisture and precipitation, *Science*, *305*, 1138–1140.

Koster, R.D., et al. (2010), The contribution of land surface initialization to subseasonal forecast skill: First results from the GLACE-2 Project, *Geophys. Res. Lett*, *37*, L02402, doi:10.1029/2009GL041677.

Lawrence, D. M., et al. (2011), Parameterization improvements and functional and structural advances in version 4 of the Community Land Model, *J. Adv. Model. Earth Syst.*, *3*, 1–27, doi:10.1029/2011MS000045.

Mueller, B., and S. I. Seneviratne (2012), Hot days induced by precipitation deficits at the global scale, *Proc. Natl. Acad. Sci. U. S. A.*, *109*(31), 12,398–12,403, doi:10.1073/pnas.1204330109.

Neale, R. B., J. Richter, S. Park, P. H. Lauritzen, S. J. Vavrus, P. J. Rasch, and M. Zhang (2013), The mean climate of the Community Atmosphere Model (CAM4) in forced SST and fully coupled experiments, *J. Clim.*, *26*(14), 5150–5168, doi:10.1175/JCLI-D-12-00236.1.

Orlowsky, B., and S. I. Seneviratne (2012), Global changes in extreme events: Regional and seasonal dimension, *Clim. Change*, *110*, 669–696, doi:10.1007/s10584-011-0122-9.

Orlowsky, B., and S. I. Seneviratne (2013), Elusive drought: Uncertainty in observed trends and short- and long-term CMIP5 projections, *Hydrol. Earth Syst. Sci.*, *17*, 1765–1781, doi:10.5194/hess-17-1765-2013.

Raddatz, T. J., C. H. Reick, W. Knorr, J. Kattge, E. Roeckner, R. Schnur, K.-G. Schnitzler, P. Wetzel, and J. Jungclaus (2007), Will the tropical land biosphere dominate the climate–carbon cycle feedback during the twenty-first century?, *Clim. Dyn.*, *29*, 565–574, doi:10.1007/s00382-007-0247-8.

Seneviratne, S. I., D. Lüthi, M. Litschi, and C. Schär (2006), Land-atmosphere coupling and climate change in Europe, *Nature*, *443*(7108), 205–209.

Seneviratne, S. I., T. Corti, E. L. Davin, M. Hirschi, E. B. Jaeger, I. Lehner, B. Orlowsky, and A. J. Teuling (2010), Investigating soil moisture–climate interactions in a changing climate: A review, *Earth Sci. Rev.*, *99*(3-4), 125–161.

Seneviratne, S. I., et al. (2012), Changes in climate extremes and their impacts on the natural physical environment, in *Managing the Risks of Extreme Events and Disasters to Advance Climate Change Adaptation*, A Special Report of Working Groups I and II of the Intergovernmental Panel on Climate Change (IPCC), edited by C. B. Field et al., pp. 109–230, Cambridge Univ. Press, Cambridge, UK, and New York, NY, USA.

Shevliakova, E., S. W. Pacala, S. Malyshev, G. C. Hurtt, P. C. D. Milly, J. P. Caspersen, L. T. Sentman, J. P. Fisk, C. Wirth, and C. Crevoisier (2009), Carbon cycling under 300 years of land use change: Importance of the secondary vegetation sink, *Global Biogeochem. Cycles*, *23*, GB2022, doi:10.1029/2007GB003176.

Shongwe, M. E., G. J. van Oldenborgh, B. J. J. M. van den Hurk, and M. A. van Aalst (2011), Projected changes in extreme precipitation in Africa under global warming, Part II: East Africa, *J. Clim.*, *24*, 3718–3733, doi:10.1175/2010JCLI2883.1.

Stevens, B., et al. (2013), Atmospheric component of the MPI-M Earth System Model: ECHAM6, *J. Adv. Model. Earth Syst.*, *5*(2), 146–172, doi:10.1002/jame.20015.

Taylor, C. M., R. A. M. De Jeu, F. Guichard, P. P. Harris, and W. A. Dorigo (2012), Afternoon rain more likely over drier soils, *Nature*, *489*, 423–426.

van den Hurk, B., M. Best, P. Dirmeyer, A. Pitman, J. Polcher, and J. Santanello (2011), Acceleration of land surface model development over a decade of GLASS, *Bull. Am. Meteorol. Soc.*, *92*(12), 1593–1600, doi:10.1175/BAMS-D-11-00007.1.

Vautard, R., P. Yiou, F. D'Andrea, N. de Noblet, N. Viovy, C. Cassou, J. Polcher, P. Ciais, M. Kageyama, and Y. Fan (2007), Summertime European heat and drought waves induced by wintertime Mediterranean rainfall deficit, *Geophys. Res. Lett.*, *34*, L07711, doi:10.1029/2006GL028001.

Wang, G. L. (2005), Agricultural drought in a future climate: Results from 15 global climate models participating in the IPCC 4th assessment, *Clim. Dyn.*, *25*, 739–753.